Acta Biomaterialia 169 (2023) 130–137

Contents lists available at ScienceDirect

Acta Biomaterialia

journal homepage: www.elsevier.com/locate/actbio

Full length article

Tissue anisotropy and collagenomics in porcine penile tunica albuginea: Implications for penile structure-function relationships and tissue engineering

Benjamin J. Bielajew[a,1], Rachel C. Nordberg[a,1], Jerry C. Hu[a], Kyriacos A. Athanasiou[a], Sriram V. Eleswarapu[b,*]

[a] Department of Biomedical Engineering, University of California Irvine, Irvine, CA, USA
[b] Department of Urology, David Geffen School of Medicine, University of California Los Angeles, Los Angeles, CA, USA

ARTICLE INFO

Article history:
Received 8 March 2023
Revised 2 August 2023
Accepted 9 August 2023
Available online 13 August 2023

Keywords:
Penis
Tunica albuginea
Corpora cavernosa
Tensile testing
Bottom-up proteomics
Penile erection
Peyronie's disease

ABSTRACT

The tunica albuginea (TA) of the penis is an elastic layer that serves a structural role in penile erection. Disorders affecting the TA cause pain, deformity, and erectile dysfunction. There is a substantial clinical need for engineered replacements of TA, but data are scarce on the material properties and biochemical composition of healthy TA. The objective of this study was to assess tissue organization, protein content, and mechanical properties of porcine TA to establish structure-function relationships and design criteria for tissue engineering efforts. TA was isolated from six pigs and subjected to histomorphometry, quantification of collagen content and pyridinoline crosslinks, bottom-up proteomics, and tensile mechanical testing. Collagen was 20 ± 2%/wet weight (WW) and 53 ± 4%/dry weight (DW). Pyridinoline content was 426 ±131 ng/mg WW, 1011 ± 190 ng/mg DW, and 45 ± 8 mmol/mol hydroxyproline. Bottom-up proteomics identified 14 proteins with an abundance of >0.1% of total protein. The most abundant collagen subtype was type I, representing 95.5 ± 1.5% of the total protein in the samples. Collagen types III, XII, and VI were quantified at 1.7 ± 1.0%, 0.8 ± 0.2%, and 0.4 ± 0.2%, respectively. Tensile testing revealed anisotropy: Young's modulus was significantly higher longitudinally than circumferentially (60 ± 18 MPa vs. 8 ± 5 MPa, $p < 0.01$), as was ultimate tensile strength (16 ± 4 MPa vs. 3 ± 3 MPa, $p < 0.01$). Taken together, the tissue mechanical and compositional data obtained in this study provide important benchmarks for the development of TA biomaterials.

Statement of Significance

The tunica albuginea of the penis serves an important structural role in physiologic penile erection. This tissue can become damaged by disease or trauma, leading to pain and deformity. Treatment options are limited. Little is known about the precise biochemical composition and biomechanical properties of healthy tunica albuginea. In this study, we characterize the tissue using proteomic analysis and tensile testing to establish design parameters for future tissue engineering efforts. To our knowledge, this is the first study to quantify tissue anisotropy and to use bottom-up proteomics to characterize the composition of penile tunica albuginea.

1. Introduction

The erectile tissue of the male penis is composed of a pair of cylindrical bodies termed the corpora cavernosa (CC) that lie along the dorsal shaft of the penis and consist of interconnected smooth muscle sinusoids lined by endothelial cells [1]. CC are surrounded by a layer of elastic tissue called the tunica albuginea (TA), which

* Corresponding author at: Department of Urology, David Geffen School of Medicine at UCLA, 10945 Le Conte Avenue, Suite 3361, Los Angeles, CA 90095, USA.
E-mail address: SEleswarapu@mednet.ucla.edu (S.V. Eleswarapu).
[1] These authors contributed equally.

https://doi.org/10.1016/j.actbio.2023.08.017

provides structural and veno-occlusive roles in physiologic erection. Disorders affecting the CC and TA can cause pain, penile deformity, and erectile dysfunction, among other problems.

In particular, Peyronie's disease (PD) is a chronic inflammatory disease involving the TA in which progressive fibrosis leads to the formation of scar tissue, termed "plaque." The etiology of PD is thought to be multifactorial and can include singular or repetitive trauma to the penis, genetic factors, inflammatory predispositions, and vascular or metabolic associations. Plaque formation as a result of fibrosis can cause pain in the acute phase of PD, followed by curvature and other deformities of the erect penis that persist in the chronic phase [2]. These plaques and deformities can have considerable impact on sexual function and the psychological and sexual wellbeing of partners. The prevalence of PD is reported to be up to 3.2% of males in the United States, and up to 20.3% of males with metabolic comorbidities [3,4]. The clinical, social, and economic consequences of PD illuminate the urgency with which suitable treatments are needed.

The therapeutic armamentarium against PD is limited. Biomaterials-based solutions for PD remain elusive and trail regenerative medicine efforts in other medical disciplines. To date, the only medication approved by the U.S. Food and Drug Administration for treatment of a PD plaque is collagenase *Clostridium histolyticum* (CCH), which works to cleave irregular amalgamations of collagen within the lesion. It is administered as an injection directly into a penile plaque over multiple appointments, followed by several weeks of mechanical stretching of the penis [5–8]. CCH has several limitations. It is a destructive therapy designed to dissolve lesions and does not provide a substrate for tissue repair or regeneration. Moreover, a full course of treatment takes approximately 28 weeks, costs upwards of $33,628, carries risks of penile hematoma and CC rupture, and achieves a maximum improvement in penile curvature that rarely exceeds 30% [5,6,8–10].

Some patients are not candidates for CCH injection therapy. These include patients with calcified plaques, wherein part or all of the plaque has become mineralized and unresponsive to collagenase digestion, as well as patients with substantial, sizable plaques that may extend irregularly into the lateral TA or septum of the TA. These latter patients are not good candidates for CCH due to the need for multiple rounds of injections and the likelihood that a course of therapy will not fully cure their disease process. For patients who are not candidates for CCH, or for those who do not respond adequately to treatment, surgery is often performed. Reconstructive surgery may employ graft materials to replace diseased TA [11]. Currently available graft materials, such as processed human pericardium or small intestinal submucosa, produce short-term improvements in penile curvature but have variable durability in long-term response, with possibility of recurrence of penile curvature, graft contracture and resultant penile shortening, erectile dysfunction, and persistent scar tissue [12].

Given the shortcomings of existing treatment modalities, as well as the vast number of individuals whose only option may be surgery, there is a clear need in the continuum of PD treatment for biomaterials-based therapies. A handful of research groups have investigated tissue engineering as a potential source of grafts for surgical treatment of PD [13–18]. Tissue engineering for PD has focused on creating sheet grafts that may be used as TA substrates during surgical reconstruction. Imbeault et al. created an autologous endothelialized tubular graft by first growing a two-dimensional fibroblast sheet, then layering endothelial cells on top [15]. Schultheiss et al. showed that the use of continuous multiaxial mechanical loading improved cell alignment and matrix infiltration in a tissue engineered model consisting of porcine fibroblasts seeded on an acellular collagen matrix [16]. Ferretti et al. performed animal testing of autologous fibroblast-seeded polyglycolic acid (PGA) scaffolds in rats; they found variations in erectile function and graft retraction depending on whether the rats received cell-seeded PGA versus empty PGA [14]. A study by Ma et al. used autologous adipose-derived stem cells (ADSCs) seeded onto small intestinal submucosa to reconstruct TA in a rat injury model; they showed advantages in penile dimensions, erectile function, and ratios of nitric oxide synthase isoforms [18].

Although these studies provide proof-of-concept for TA tissue engineering, they are motivated primarily by histological and engraftment considerations, rather than by recapitulation of the intrinsic functional properties of TA. A precise understanding of the functional properties of TA is critical to tissue engineering efforts, since TA must endure substantial mechanical forces during physiologic penile erection and sexual activity. Unfortunately, there is a paucity of data on the material properties and biochemical composition of healthy TA. Mass spectrometry-based bottom-up proteomic techniques have recently emerged as a quantification tool for matrix components of biological tissues [19,20]. Recent advancements have enabled the quantification of individual collagen subtypes, which play unique roles in providing structure and mechanical properties to soft tissues [21]. While gene expression of collagen subtypes has previously been studied in the TA [22], no studies to date have determined the quantities or ratios of collagen subtypes in TA matrix. This study employs bottom-up proteomics to investigate the matrix composition and collagen subtype quantities in porcine TA. Further, to translate a tissue-engineered implant to clinical use, an animal model must be established in order to assess the safety and efficacy *in vivo* [23]. Therefore, the objective of this study was to assess tissue organization, protein content, and mechanical properties of porcine TA to establish structure-function relationships, derive native tissue functional properties for TA in a prospective preclinical model, and provide precise design criteria for future TA tissue engineering efforts.

2. Materials and methods

2.1. Tissue isolation

Porcine penises ($n = 6$) were collected from sexually mature male domestic farm pigs that had been culled by an abattoir for reasons unrelated to the current study (tissue procured by Sierra for Medical Science, Whittier, CA). Of note, porcine penis consists of one corpus cavernosum, in contrast to the paired corpora cavernosa present in the human penis. The porcine penis dissection process is shown in Fig. 1**A.** Briefly, the skin and urethra were removed via dissection with a scalpel to produce TA-CC units. For histology, cross sections of TA-CC units were fixed in 10% neutral-buffered formalin for at least 72 h. The dorsal TA was further isolated from surrounding tissue via dissection with a scalpel and tenotomy scissors, and 3 adjacent TA specimens (approximately 2 cm x 1 cm) were isolated from each penis for a total of 18 samples (i.e., $n == 6$ with 3 replicates per penis). As depicted in Fig. 1**B**, these samples were divided into pieces for uniaxial tensile testing, biochemical assays, crosslinks analysis, and bottom-up proteomics.

2.2. Histology

Formalin-fixed samples were embedded in paraffin wax and sectioned at a thickness of 7 μm using a microtome. The sections were mounted on SuperFrost Plus glass slides (VWR, Radnor, PA) and stained via hematoxylin and eosin (H&E). Slides were imaged with a Ventana DP-200 slide scanner (Roche, Basel, Switzerland). Dimensions of the dorsal and ventral TA walls were measured by ImageJ analysis of $n == 6$ samples. Additionally, samples were stained using picrosirius red and imaged via brightfield and polarized light microscopy with a Nikon Eclipse Te2000 inverted fluorescence microscope (Nikon, Minato City, Tokyo, Japan).

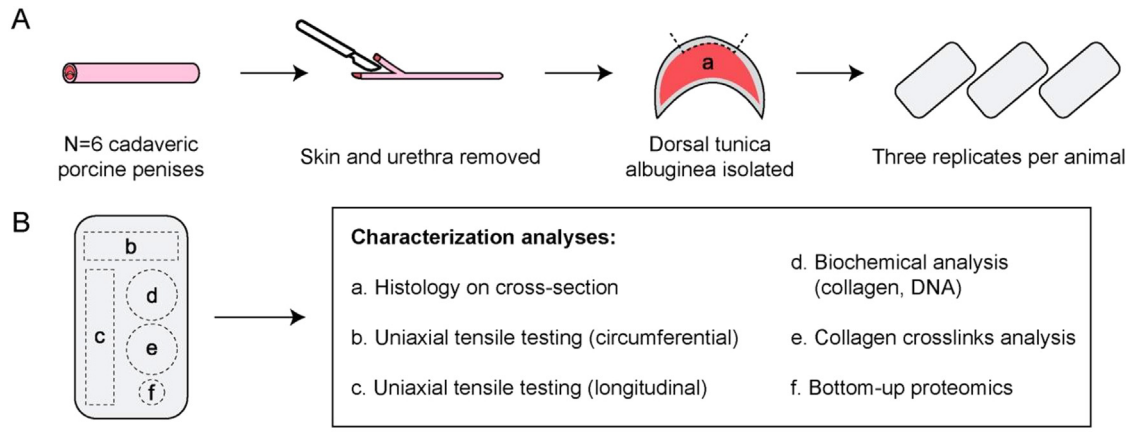

Fig. 1. Sample collection and characterization assays. (A) Process for collection of tunica albuginea samples from cadaveric porcine penises. (B) Tunica albuginea tissues were further divided into samples for mechanical, biochemical, and proteomic characterizations. Histology was performed on the intact tunica albuginea and corpus cavernosum units.

2.3. Biochemical assays

For biochemical analysis of collagen and DNA, TA wet weights (WWs) were taken after isolation, then samples were lyophilized, and dry weights (DWs) were measured. Samples were digested in papain to produce a homogeneous digest. To quantify collagen, a hydroxyproline assay was performed, as previously described [24]. DNA was quantified with a Quant-iT^{TM} PicoGreen^{TM} dsDNA Assay Kit, following manufacturer's instructions. Collagen and DNA measurements were normalized to WW and DW.

2.4. Collagen crosslinks and bottom-up proteomics

Collagen crosslinks analysis and bottom-up proteomics were performed, as previously described [21]. Briefly, WW and DW were taken on crosslinks samples, and then they were hydrolyzed in 6 N hydrochloric acid overnight, filtered, and analyzed using a liquid chromatography–mass spectrometry assay targeted to the masses of pyridinoline (PYR) and hydroxyproline (OHP). These compounds were selected because pyridinoline is the most common mature enzymatic crosslink in collagenous tissue, and hydroxyproline serves as an additional normalization to weight (i.e., PYR/OHP represents how crosslinked the collagen is in the tissue). PYR content was normalized to WW, DW, and OHP. Bottom-up proteomics is an analysis that performs quantification on peptide digests using mass spectrometry and database searching to yield protein contents in tissues. Samples were digested overnight in mass spectrometry grade trypsin, desalted, and analyzed on a Thermo Fisher Scientific Orbitrap Fusion Lumos mass spectrometer, followed by label-free quantification using MaxQuant software [25]. All quantification values are represented as target protein per total protein (%/PROT). Only proteins with greater than 0.1%/PROT in at least one sample were reported. A threshold of 0.1% was chosen to pare down the list of 270 proteins to 14. These 14 represent, on average, 99.5% of the total protein mass of the TA samples.

2.5. Tensile testing

For tensile testing, each specimen was tested along both the longitudinal and circumferential axes. Dog-bone shaped specimens were cut from the TA in each direction using a scalpel to extract the tissue and a biopsy punch to cut the tissue into a dog bone conformation. The specimens were then photographed, and the cross-sectional area of each specimen was determined via ImageJ analysis. Samples were tested in uniaxial strain using an Instron 5565 (Instron, Norwood, MA) and a 5000 N load cell (serial number Instron UK964). Samples were subjected to a preload of 0.2 N before testing. Gauge length of the sample was measured after preloading the sample. The specimens were pulled at a rate of 1% gauge length per second until catastrophic failure. A linear elastic model was used to analyze the data. Force-displacement curves were used to generate stress-strain curves. The stress-strain curves were utilized to calculate the tensile Young's modulus, ultimate tensile strength (UTS), strain at failure, resilience, and toughness using MATLAB. The Young's modulus was calculated from the linear portion of the stress-strain curve. Anisotropy index was calculated by dividing the values of the longitudinal axis over the circumferential axis, based on a method previously utilized to quantify anisotropy in tissue-engineered meniscal tissue [26,27].

2.6. Statistical analysis

For tensile, biochemical, and crosslinks data, triplicate samples isolated from the same animal were used as technical replicates. Shapiro-Wilk tests were utilized to verify the normality of the mechanical testing data. Data sets that passed the Shapiro-Wilk test were analyzed with a paired Student's t-test, and those that did not pass were analyzed with a Wilcoxon test ($n == 6$ per group, $p < 0.05$). All data in bar graphs are presented as means with error bars representing the standard deviation. Pie chart values for proteomics results are means.

3. Results

3.1. Histology and histomorphometry

H&E stain was used to visualize and assess tissue organization of the TA and the enclosed CC tissue (Fig. 2A). The dorsal (Fig. 2B) and ventral (Fig. 1C) TA walls were morphologically distinct. The dorsal wall was 0.6 ± 0.1 mm in thickness and organized into clusters, whereas the ventral wall was 0.4 ± 0.1 mm in thickness and homogeneous in structure. The thickness of the ventral TA wall was significantly thinner than the dorsal TA wall ($p < 0.05$). In terms of tissue organization, the porcine TA displayed an undulating fiber arrangement, which has been previously described in the human [28]. Picrosirius red staining demonstrated that the tissue was rich in collagen (Fig. 1D,E). Moderate collagen alignment was observed via polarized light microscopy in the dorsal-ventral axis (Fig. 2F,G).

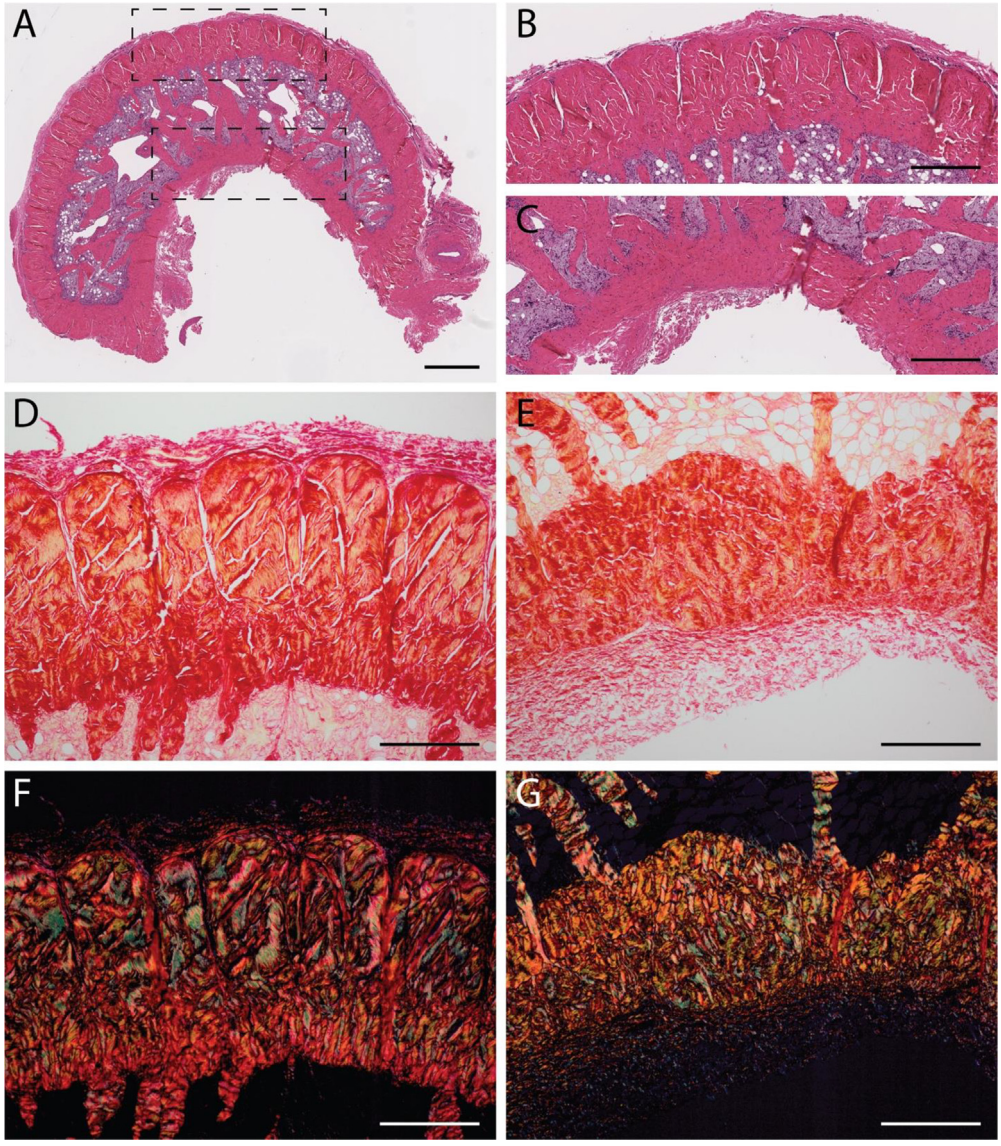

Fig. 2. Histology of porcine tunica albuginea and corpus cavernosum. (A) Representative Hematoxylin and Eosin staining of entire tunica albuginea and corpus cavernosum unit (scale bar = 800 μm). Dashed boxes indicate magnified image location. Magnified images of (B) the dorsal tunica albuginea wall (scale bar = 400 μm) and (C) the ventral tunica albuginea wall (scale bar = 400 μm). Picrosirius red staining of (D) the dorsal tunica albuginea wall (scale bar = 400 μm) and (E) the ventral tunica albuginea wall (scale bar = 400 μm). Polarized light microscopy of the (F) the dorsal tunica albuginea wall (scale bar = 400 μm) and (G) the ventral tunica albuginea wall (scale bar = 400 μm). In the polarized light microscopy images (F-G), aligned collagen type I fibers appear red-yellow, while thinner fibers, including those made of collagen type III, appear green [41,42].

3.2. Biochemical assays and collagen crosslinks

The hydration of the TA, from the ratio of WW to DW, was calculated to be 63 ± 2%. Collagen content was 20 ± 2%/WW and 53 ± 4%/DW. DNA content was 0.05 ± 0.01%/WW and 0.14 ± 0.02%/DW. PYR content of the TA was determined to be 425 ±131 ng/mg WW, 1011 ± 190ng/mg DW, and 45 ± 8 mmol/mol OHP. All biochemical and crosslinks results are displayed in Fig. 3.

3.3. Tensile testing

Results of tensile testing are presented in Fig. 4. Tensile testing of the dorsal wall of the TA indicated that anisotropy was present within the tissue. The Young's modulus was significantly higher along the longitudinal axis at 60 ± 18 MPa than in the circumferential axis at 8 ± 5 MPa ($p < 0.01$). The anisotropy index of the Young's modulus was calculated to be 7. The UTS of the tissue was also significantly higher along the longitudinal axis than along the circumferential axis with values of 16 ± 4 MPa and 3 ± 3 MPa, respectively ($p < 0.01$). The anisotropy index of the UTS modulus was calculated to be 4.6. However, the strain at failure was not significantly affected by testing direction with values of 0.7 ± 0.3 along the longitudinal axis and 0.7 ± 0.5 in the circumferential axis. Resilience of the longitudinal axis was significantly higher ($p < 0.05$) than resilience along the circumferential axis at 4 ± 2 and 1 ± 1, respectively. Toughness along the longitudinal axis was not significantly higher than toughness in the circumferential axis at 7 ± 2 and 3 ± 3, respectively.

3.4. Bottom-up proteomics

Label-free quantification resulted in 270 total proteins detected in the porcine TA samples. However, upon removing all protein results that were less than 0.1%/PROT in at least one sample, only 14 proteins were left. These 14 proteins, shown in Fig. 5, represent 99.5 ± 0.2% of the protein in the TA samples. In the

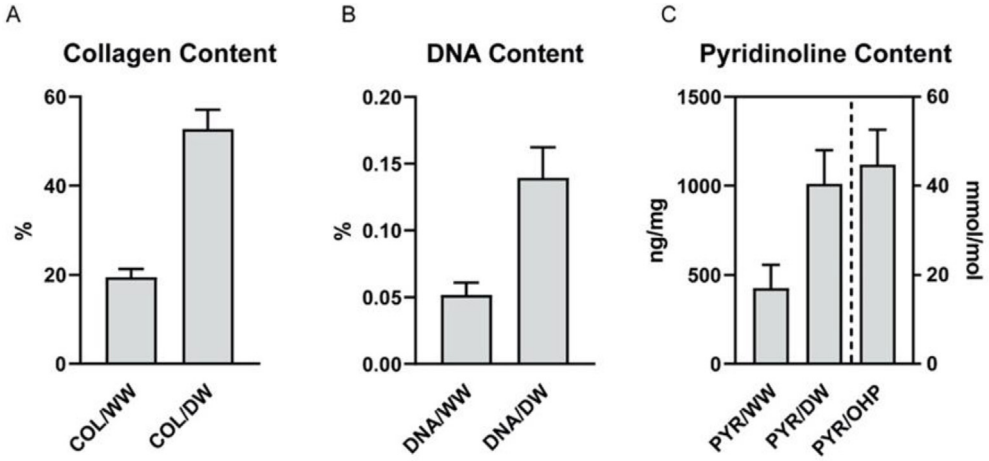

Fig. 3. Biochemical and crosslink properties of porcine tunica albuginea (n == 6). (A) collagen content (COL) normalized to wet weight (WW) and dry weight (DW). (B) DNA content normalized to WW and DW. (C) Pyridinoline content (PYR) normalized to WW, DW, and hydroxyproline (OHP). The hydration of the tissue was calculated to be 62.99% ± 2.36%. Error bars represent standard deviation.

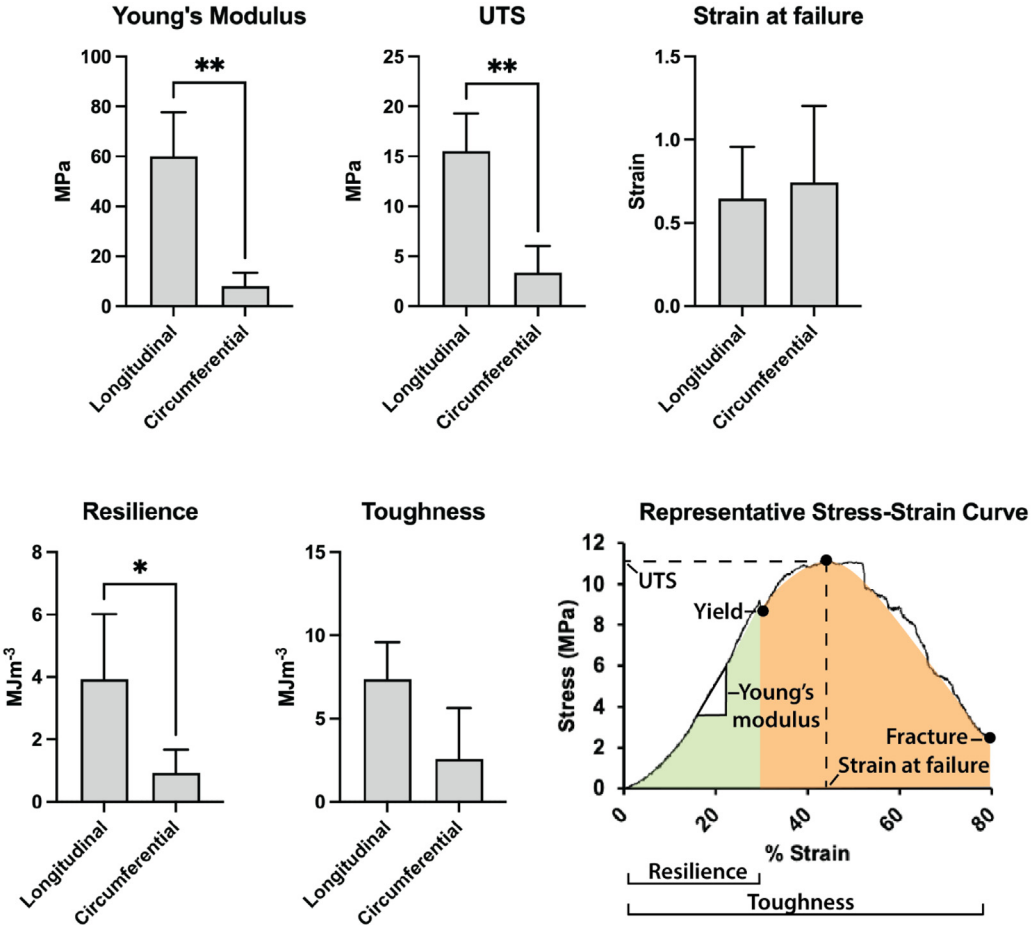

Fig. 4. Tensile properties of porcine tunica albuginea (n == 6). Young's modulus, ultimate tensile stress (UTS), strain at failure, resilience, and toughness of tunica albuginea tested along the longitudinal and circumferential axes (* $p < 0.05$, ** $p < 0.01$). Error bars represent standard deviation. A representative stress-strain curve is provided, showing the different results acquired from the tensile tests; Young's modulus is the slope of the linear portion of the stress-strain curve, UTS is the greatest stress in the curve, strain at failure is the strain at tissue fracture, resilience is the area under the curve to the yield point, and toughness is the area under the curve to fracture.

graph, COL1 contains two proteins (alpha-1, alpha-2), COL5 contains two proteins (alpha-1, alpha-2), and COL6 contains two proteins (alpha-2, alpha-3). Most of the proteomic composition of the TA is collagen, accounting for 98.5% of the total protein content. The most abundant collagen subtype is collagen type I, which represented 95.5 ± 1.5% of the total protein in the samples. Other collagen types, including type III, type XII, and type VI were quantified at 1.7 ± 1.0%/PROT, 0.8 ± 0.2%/PROT, and 0.4 ± 0.2%/PROT, respectively. The non-collagen proteins comprise albumin (ALBU, 0.5% ± 0.2%), hemoglobin subunit alpha (HBA, 0.2% ± 0.1%), vimentin (VIME, 0.1% ± 0.1%), cytoplasmic actin 1 (ACTB, 0.1% ± 0.1%), and ig lambda chain C region (LAC,

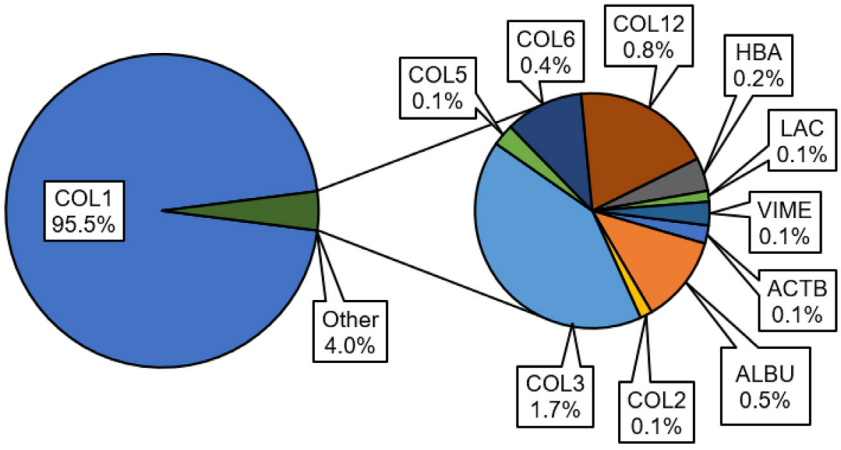

Fig. 5. Bottom-up proteomics analysis of porcine tunica albuginea ($n == 6$). Mean values are reported as percent protein per total protein content. COL1, collagen type I. COL2, collagen type II. COL3, collagen type III. COL5, collagen type V. COL6, collagen type VI. COL12, collagen type XII. HBA, hemoglobin subunit alpha. LAC, Ig lambda chain C region. VIME, vimentin. ACTB, Cytoplasmic actin. ALBU, albumin.

0.1% ± 0.0%). A full list of 270 proteins quantified by bottom-up proteomics is in **Supplementary Table 1.**

4. Discussion

The objective of this study was to assess the functional properties of porcine TA in terms of tissue organization, protein content, and mechanical properties. These data will aid in the understanding of structure-function relationships of the TA and provide design criteria for future TA tissue engineering endeavors, which remain an elusive but critical need for the treatment of penile deformity.

To our knowledge, this is the first study to report tensile properties of the porcine TA and quantify the anisotropy inherent to TA. Young's modulus values of the porcine TA ranged from 8.1-60.0 MPa. For comparison, these values are lower than those reported in the menisci (e.g., Young's modulus values ranged from 78.4–116.2 MPa in minipig menisci [27]). However, these values are close in range with those reported in hyaline cartilage tissue (e.g., Young's modulus values range from 7.0-32.5 MPa in human knee cartilage [29] and 6.7-20.3 MPa in minipig facet joint cartilage [30]). Similarly, decellularized human pericardium, which is used selectively in some TA reconstructive approaches in penile surgery, has been reported to have a Young's modulus of approximately 28MPa [31]. The porcine TA displayed highly anisotropic behavior when tested in tension. The Young's modulus and UTS values were significantly higher along the longitudinal direction than along the circumferential direction. This is consistent with previous studies in a primate model, which reported a Young's modulus of 26.4 MPa longitudinally and 11.9 MPa circumferentially and a UTS of 3.8 MPa longitudinally and 1.9 MPa circumferentially [32]. The anisotropy index values in the porcine TA were relatively high at 7.4 Young's modulus and 4.6 UTS. For comparison, the highly anisotropic tissue of the meniscus had an anisotropy index of 11.2–49.4 for the Young's modulus and 6.3–11.2 for the UTS in a minipig model [27]. In terms of tissue engineering applications, the anisotropy index values of tissue-engineered neomenisci for orthopaedic applications were reported to be approximately 4 and 2.5 for Young's modulus and UTS, respectively [26]. Altogether, anisotropy appears to be a characteristic that is preserved across species and may be a key design consideration for the generation of tissue-engineered TA replacements.

The Young's modulus, UTS, strain at failure, resilience, and toughness of porcine TA serve as important benchmarks for future urogenital biomaterials development. Prior work in this area is scant in the published literature. In 1990, Bitsch et al. measured TA elasticity in cadaveric human penises using three indirect methods: saline infusion until rupture, measurement with tensiometer, and progressive inflation of a penile prosthesis until herniation. Despite the limitations inherent to indirect measurement of these material properties, and without consideration of tissue anisotropy, a median UTS of 100 kPa was reported [28]. In a subsequent study by Hsu et al. in 1994, in order to understand penile prosthesis extrusion, a mechanical force gauge was modified to simulate a penile prosthesis, and the force required to penetrate tunica albuginea was measured [33]. Maximal breaking point pressure was 45 MPa. The indirect measurements of TA elasticity from these two early studies provide context for the present study and motivate further work to establish TA material properties across species. One limitation of this study is that preconditioning was not applied prior to tensile testing, which could influence the viscoelastic behavior of the tissue; future work using viscoelastic models for mechanical testing will be necessary to fully interrogate the viscoelastic behavior of the TA.

Bottom-up proteomics has recently been highlighted as a powerful tool for tissue characterization [19,20]. The present study represents, to our knowledge, the first usage of bottom-up proteomics for characterizing the TA. The TA is comprised mostly of collagen, which represents 98.51% of the total protein content of the tissue; almost all of which is collagen type I. This high collagen type I ratio is often seen in tissues that are required to function under high tensile stresses and strains, such as ligaments, tendons, skin, and fibrocartilages [20]. The ratio of collagen type I to collagen type III in the TA is about 58:1, which is much higher than other tissues, for example, skin, which has a ratio of 4:1 [34], or red-red meniscus, which has a ratio of 16:1 [21]. There has not yet been enough collagen subtype quantification performed to determine what it this high ratio in the TA means in terms of functionality, but future proteomic work in more biological tissues, as well as more proteomics studies on the TA in healthy and diseased states may further understanding. Interestingly, a small proportion of collagen type II was found in the TA, even though this collagen type is very rarely found in tissues that are not cartilage. There were some non-collagen proteins that were present at levels at or above 0.1% in the TA. These were cytoskeletal constituents such as actin and vimentin, and proteins found in blood such as albumin, hemoglobin subunit a, and immunoglobin lambda chain. It is possible that proteins of low abundances (<0.1%) can have significant functional consequences, and the full set of proteins in **Supplementary Table 1** should be considered when engineering functional replacement tissues. One limitation of the bottom-up proteomics ap-

proach in this work is that elastin is not readily quantifiable in this analysis due its crosslinked structure, which limits the available lysine and arginine residues for trypsin digestions. Future studies on TA that quantify elastin, as well as non-protein matrix components, such as glycosaminoglycans, which have previously been found in TA [35,36], will augment understanding of how specific matrix macromolecules relate to TA mechanical properties and disease states. It should be noted that the biochemistry assay for collagen content only detected 52% collagen by dry weight. Therefore, the rest of the matrix may consist of elastin or other components such as glycosaminoglycans, cellular membranes, lipids, metabolites, or nucleic acids. By fully defining the composition of TA matrix, benchmarks for engineered tissue biochemistry will be developed toward designing functional replacement tissues.

Additionally, to our knowledge, this is the first study to quantify pyridinoline crosslinks within penile tunica albuginea. Crosslinking of collagen is a major post-translational modification of collagen that influences biomechanical integrity. This study showed that the collagen of porcine TA is highly crosslinked, with PYR/OHP values over double that of fibrocartilages and hyaline cartilages, though, due to comparatively lower overall collagen content, the PYR/DW values were on par with hyaline cartilages and less than most fibrocartilages [21]. Pyridinoline crosslinks have been shown to correlate with both tensile stiffness and strength in orthopaedic tissues [37,38], but there is a dearth of literature describing the contribution of pyridinoline crosslinks to the mechanical behavior of penile erectile tissue. Specifically, it would be of great interest to urological researchers to determine the role of pyridinoline crosslinks in Peyronie's disease, given that scars in other tissues (e.g., skin) can be associated with increased levels of enzymatic crosslinks [39]. Furthermore, the results from this study can inform future tissue engineering efforts that aim to reproduce the biochemical composition of native tunica albuginea. Strategies to increase collagen crosslinking, for example through lysyl oxidase or growth factor stimuli, could play a role in such efforts. Additional collagen crosslinks, such as immature pyridinoline and non-enzymatic crosslinks such as glucosepane and pentosidine, will be important to study in future TA characterization efforts.

Structure-function relationships of matrix components of the TA (e.g., the relationship of collagen content and organization to tensile properties) will continue to be studied in future proteomic analyses of healthy and diseased TA tissues. Furthermore, the mechanical role of minor collagen types (i.e., collagen types II, III, V, VI, and XII) can be better elucidated in the future with knockout models, spatialization techniques (e.g., immunohistochemistry), and by studying the proteomic composition and mechanical properties of diseased tissues, in which derangements of the ratios of collagen subtypes may be implicated. For example, mutations in the Col12a1 gene show muscle weakness and joint hyperlaxity [40], but mechanical properties of collagenous tissues such as the TA are not yet known.

At the present time, there is no adequate animal model for TA tissue engineering efforts. Animal models larger than rodents, such as porcine models or leporine models, are thought to be more appropriate, given the more robust size of the penis in these latter animals. We elected to study porcine tissue given animal availability, size of the penis for testing, and morphological similarities of the CC and TA to human histology, although we do acknowledge limitations inherent in a singular CC model versus the human model's paired CC. A limitation of the porcine model is that the porcine penis consists of a single corpus cavernosum, rather than the paired CC present in the human penis. Despite this difference in anatomical arrangement, the principles of erectile function remain the same, with arterial filling of the cavernosal sinusoids and TA-driven occlusion of venous drainage. Pre-clinical studies on tissue engineered TA substitutes will require adequate animal models for testing and evaluation, and the data herein establish benchmarks for work in a potential porcine model. The work described in our manuscript represents a first step in evaluating species-specific characteristics of TA. Future work will enumerate interspecies differences (e.g., pig versus rabbit) and human characteristics (cadaveric versus live healthy versus live diseased).

5. Conclusions

Taken together, the tissue mechanical and compositional data obtained in this study provide important benchmarks for the development of TA biomaterials for the treatment of Peyronie's disease or other deformities of the penis. These data may also inform the development of animal models to study biologic interventions on Peyronie's disease plaques. Further interspecies comparisons (e.g., porcine versus human TA) are warranted.

Data availability

All data collected for this study is available from the corresponding author upon reasonable request.

Declaration of Competing Interest

The authors declare that they have no known competing financial interests or personal relationships that could have appeared to influence the work reported in this paper.

Acknowledgments

Funding: This work was supported in part by the American Urological Association and Urology Care Foundation (Research Scholar Award to SVE). This work was also supported by NIH TL1 TR001415 (RCN).

Supplementary materials

Supplementary material associated with this article can be found, in the online version, at doi:10.1016/j.actbio.2023.08.017.

References

[1] D. Prieto, Physiological regulation of penile arteries and veins, Int. J. Impot. Res. 20 (2008) 17–29, doi:10.1038/SJ.IJIR.3901581.
[2] K.L. Sharma, M. Alom, L. Trost, The etiology of peyronie's disease: pathogenesis and genetic contributions, Sex. Med. Rev. 8 (2020) 314–323, doi:10.1016/J.SXMR.2019.06.004.
[3] D.B. Dibenedetti, D. Nguyen, L. Zografos, R. Ziemiecki, X. Zhou, A population-based study of Peyronie's disease: prevalence and treatment patterns in the United States, Adv. Urol. (2011) 2011, doi:10.1155/2011/282503.
[4] K.A. Ostrowski, J.R. Gannon, T.J. Walsh, A review of the epidemiology and treatment of Peyronie's disease, Res. Reports Urol. 8 (2016) 61, doi:10.2147/RRU.S65620.
[5] M. Gelbard, I. Goldstein, W.J.G. Hellstrom, C.G. McMahon, T. Smith, J. Tursi, N. Jones, G.J. Kaufman, C.C. Carson, Clinical efficacy, safety and tolerability of collagenase clostridium histolyticum for the treatment of peyronie disease in 2 large double-blind, randomized, placebo controlled phase 3 studies, J. Urol. 190 (2013) 199–207, doi:10.1016/J.JURO.2013.01.087.
[6] L.I. Lipshultz, I. Goldstein, A.D. Seftel, G.J. Kaufman, T.M. Smith, J.P. Tursi, A.L. Burnett, Clinical efficacy of collagenase Clostridium histolyticum in the treatment of Peyronie's disease by subgroup: results from two large, double-blind, randomized, placebo-controlled, phase III studies, BJU Int. 116 (2015) 650–656, doi:10.1111/BJU.13096.
[7] N.M. Haney, T.P. Kohn, P.E. Nichols, W.J.G. Hellstrom, The effect of adjunct mechanical traction on penile length in men undergoing primary treatment for Peyronie's disease: a systematic review and meta-analysis, Urology 122 (2018) 110–115, doi:10.1016/J.UROLOGY.2018.07.039.
[8] A. Amighi, S.A. Mills, S.V. Eleswarapu, K.V. Regets, N. Mendhiratta, J.N. Mills, A modified technique for intralesional injection of collagenase Clostridium histolyticum for Peyronie's disease results in reduced procedural morbidity using a standardized hematoma classification rubric, World J. Urol. 38 (2020) 293–298, doi:10.1007/S00345-019-02812-9.

[9] K. Wymer, T. Kohler, L. Trost, Comparative cost-effectiveness of surgery, collagenase clostridium histolyticum, and penile traction therapy in men with Peyronie's disease in an era of effective clinical treatment, J. Sex. Med. 16 (2019) 1421–1432, doi:10.1016/J.JSXM.2019.06.010.
[10] D.T. Walker, R.H. Shahinyan, A. Amighi, K.V. Regets, J.N. Mills, S.V. Eleswarapu, Impact of treatment-related adverse events on efficacy of intralesional collagenase therapy for Peyronie's disease, Int. J. Impot. Res. 33 (2021) 128–130, doi:10.1038/S41443-020-0311-Z.
[11] G. Hatzichristodoulou, D. Osmonov, H. Kübler, W.J.G. Hellstrom, F.A. Yafi, Contemporary review of grafting techniques for the surgical treatment of Peyronie's disease, Sex. Med. Rev. 5 (2017) 544–552, doi:10.1016/J.SXMR.2017.01.006.
[12] J.L. Almeida, J. Felício, F.E. Martins, Surgical planning and strategies for Peyronie's disease, Sex. Med. Rev. 9 (2021) 478–487, doi:10.1016/J.SXMR.2020.07.008.
[13] D. Eberli, R. Susaeta, J.J. Yoo, A. Atala, Tunica repair with acellular bladder matrix maintains corporal tissue function, Int. J. Impot. Res. 19 (2007) 602–609, doi:10.1038/sj.ijir.3901587.
[14] L. Ferretti, M. Giuliani, T. Bessède, X. Qiu, H. Zhang, B. Alsaid, A. Durrbach, F. Giuliano, G. Benoit, S. Droupy, Tissue engineering for penile surgery: comparative study of noncellular and cell-seeded synthetic grafts for tunica albuginea replacement, J. Sex. Med. 9 (2012) 625–631, doi:10.1111/J.1743-6109.2011.02561.X.
[15] A. Imbeault, G. Bernard, G. Ouellet, S. Bouhout, S. Carrier, S. Bolduc, Surgical option for the correction of Peyronie's disease: an autologous tissue-engineered endothelialized graft, Undefined 8 (2011) 3227–3235, doi:10.1111/J.1743-6109.2011.02374.X.
[16] D. Schultheiss, R.R. Lorenz, R. Meister, M. Westphal, A.I. Gabouev, H. Mertsching, C. Biancosino, N. Schlote, J. Wefer, M. Winkler, C.G. Stief, U. Jonas, Functional tissue engineering of autologous tunica albuginea: a possible graft for Peyronie's disease surgery, Eur. Urol. 45 (2004) 781–786, doi:10.1016/j.eururo.2004.01.001.
[17] H.S. Yu, J. Park, H.-S. Lee, S.A. Park, D.-W. Lee, K. Park, Feasibility of polycaprolactone scaffolds fabricated by three-dimensional printing for tissue engineering of Tunica Albuginea, World J. Mens. Health. 36 (2018) 66, doi:10.5534/WJMH.17025.
[18] L. Ma, Y. Yang, S.C. Sikka, P.J. Kadowitz, L.J. Ignarro, A.B. Abdel-Mageed, W.J.G. Hellstrom, Adipose tissue-derived stem cell-seeded small intestinal submucosa for tunica albuginea grafting and reconstruction, Proc. Natl. Acad. Sci. U. S. A. 109 (2012) 2090–2095, doi:10.1073/PNAS.1113810109.
[19] B.J. Bielajew, R.P. Donahue, E.K. Lamkin, J.C. Hu, V.C. Hascall, K.A. Athanasiou, Proteomic, mechanical, and biochemical characterization of cartilage development, Acta Biomater. 143 (2022) 52–62, doi:10.1016/J.ACTBIO.2022.02.037.
[20] B.J. Bielajew, J.C. Hu, K.A. Athanasiou, Collagen: quantification, biomechanics and role of minor subtypes in cartilage, Nat. Rev. Mater. 5 (2020) 730–747, doi:10.1038/s41578-020-0213-1.
[21] B.J. Bielajew, J.C. Hu, K.A. Athanasiou, Methodology to quantify collagen subtypes and crosslinks: application in minipig cartilages, Cartilage 13 (2021) 1742S–1754S, doi:10.1177/19476035211060508.
[22] E.J.P.M. ten Dam, M.F. van Driel, I.J. de Jong, P.M.N. Werker, R.A. Bank, Glimpses into the molecular pathogenesis of Peyronie's disease, Aging Male 23 (2020) 962–970, doi:10.1080/13685538.2019.1643311.
[23] R.C. Nordberg, G.A. Otarola, D. Wang, J.C. Hu, K.A. Athanasiou, Navigating regulatory pathways for translation of biologic cartilage repair products, Sci. Transl. Med. 14 (2022) eabp8163, doi:10.1126/SCITRANSLMED.ABP8163/SUPPL_FILE/SCITRANSLMED.ABP8163_SM.PDF.
[24] D.D. Cissell, J.M. Link, J.C. Hu, K.A. Athanasiou, A modified hydroxyproline assay based on hydrochloric acid in Ehrlich's solution accurately measures tissue collagen content, Tissue Eng. Part C 23 (2017) 243–250, doi:10.1089/ten.tec.2017.0018.
[25] J. Cox, M. Mann, MaxQuant enables high peptide identification rates, individualized p.p.b.-range mass accuracies and proteome-wide protein quantification, Nat. Biotechnol. 26 (2008) 1367–1372, doi:10.1038/nbt.1511.
[26] E.A. Gonzalez-Leon, B.J. Bielajew, J.C. Hu, K.A. Athanasiou, Engineering self-assembled neomenisci through combination of matrix augmentation and directional remodeling, Acta Biomater. 109 (2020) 73–81, doi:10.1016/j.actbio.2020.04.019.
[27] E.A. Gonzalez-Leon, J.C. Hu, K.A. Athanasiou, Yucatan minipig knee meniscus regional biomechanics and biochemical structure support its suitability as a large animal model for translational research, Front. Bioeng. Biotechnol. (2022) 10, doi:10.3389/FBIOE.2022.844416.
[28] M. Bitsch, B. Kromann-Andersen, J. Schou, E. Sjontoft, The elasticity and the tensile strength of tunica albuginea of the corpora cavernosa, J. Urol. 143 (1990) 642–645, doi:10.1016/S0022-5347(17)40047-4.
[29] E.Y. Salinas, G.A. Otarola, H. Kwon, D. Wang, J.C. Hu, K.A. Athanasiou, A.K. Salinas E, G Otarola, H Kwon, D Wang, J Hu, Topographical characterization of the young, healthy human femoral medial condyle, Cartilage (2022), doi:10.1177/19476035221141421.
[30] R.C. Nordberg, A.N. Kim, J.M. Hight, R.S. Meka, B.D. Elder, J.C. Hu, K.A. Athanasiou, Biochemical and biomechanical characterization of the cervical, thoracic, and lumbar facet joint cartilage in the Yucatan minipig, J. Biomech. 142 (2022) 111238, doi:10.1016/J.JBIOMECH.2022.111238.
[31] L. Wollmann, P. Suss, J. Mendonça, C. Luzia, A. Schittini, G.W.X. da Rosa, F. Costa, F.F. Tuon, Characterization of decellularized human pericardium for tissue engineering and regenerative medicine applications, Arq. Bras. Cardiol. 113 (2019) 11–17, doi:10.5935/abc.20190094.
[32] A.M. Kandabarow, E. Chuang, K. McKenna, B. Le, K. McVary, A. Colombo, Tensile strength of penile tunica albuginea in a primate model, J. Urol. (2021) 206, doi:10.1097/JU.0000000000002099.04.
[33] G.L. Hsu, G. Brock, L. Martinez-Pineiro, B. Von Heyden, T.F. Lue, E.A. Tanagho, Anatomy and strength of the tunica albuginea: its relevance to penile prosthesis extrusion, J. Urol. 151 (1994) 1205–1208, doi:10.1016/S0022-5347(17)35214-X.
[34] W.K. Stadelmann, A.G. Digenis, G.R. Tobin, Physiology and healing dynamics of chronic cutaneous wounds, Am. J. Surg. 176 (1998) 26S–38S, doi:10.1016/S0002-9610(98)00183-4.
[35] K. Shiina, Collagen and acid glycosaminoglycans in bovine tunica albuginea during ovulatory cycle, Nihon Sanka Fujinka Gakkai Zasshi 42 (1990) 1510–1517.
[36] A.L. Bastos, F.J.B. Sampaio, L.E.M. Cardoso, Compositional changes of collagen and glycosaminoglycans in the tunica albuginea and corpus cavernosum from the human penis during the fetal and postnatal periods, J. Urol. 173 (2005) 1039–1043, doi:10.1097/01.JU.0000145592.32180.24.
[37] A.K. Williamson, A.C. Chen, K. Masuda, E.J.M.A. Thonar, R.L. Sah, Tensile mechanical properties of bovine articular cartilage: variations with growth and relationships to collagen network components, J. Orthop. Res. 21 (2003) 872–880, doi:10.1016/S0736-0266(03)00030-5.
[38] S.V. Eleswarapu, D.J. Responte, K.A. Athanasiou, Tensile properties, collagen content, and crosslinks in connective tissues of the immature knee joint, PLoS One 6 (2011), doi:10.1371/JOURNAL.PONE.0026178.
[39] K.C. Wan, W.H. Lewis, Study of free iron and pyridinoline in hypertrophic scars and normal skin, Br. J. Biomed. Sci. 53 (1996) 196–203 https://pubmed.ncbi.nlm.nih.gov/8914346/. (Accessed 24 February 2023).
[40] Y. Zou, D. Zwolanek, Y. Izu, S. Gandhy, G. Schreiber, K. Brockmann, M. Devoto, Z. Tian, Y. Hu, G. Veit, M. Meier, J. Stetefeld, D. Hicks, V. Straub, N.C. Voermans, D.E. Birk, E.R. Barton, M. Koch, C.G. Bönnemann, Recessive and dominant mutations in COL12A1 cause a novel EDS/myopathy overlap syndrome in humans and mice, Hum. Mol. Genet. 23 (2014) 2339–2352, doi:10.1093/HMG/DDT627.
[41] J. Liu, M.-Y. Xu, J. Wu, H. Zhang, L. Yang, D.-X. Lun, Y.-C. Hu, B. Liu, Picrosirius-polarization method for collagen fiber detection in tendons: a mini-review, Orthop. Surg. 13 (2021) 701–707, doi:10.1111/os.12627.
[42] L.C. Junqueira, W. Cossermelli, R. Brentani, Differential staining of collagens type I, II and III by Sirius Red and polarization microscopy, Arch. Histol. Jpn. 41 (1978) 267–274, doi:10.1679/aohc1950.41.267.